Detecting the effects of inter-annual and seasonal changes in environmental factors on the striped red mullet population in the Bay of Biscay

Claire Kermorvant, Nathalie Caill-Milly, Damien Sous, Iosu Paradinas, Muriel Lissardy, Benoit Liquet

Version of Record: https://www.sciencedirect.com/science/article/pii/S1385110121000149
Manuscript_10421c4007209c488d8b2cb79437c51d

Detecting the effects of inter-annual and seasonal changes in environmental factors on the striped red mullet population in the Bay of Biscay

Claire Kermorvant[a,b], Nathalie Caill-Milly[c], Damien Sous[d,e], Iosu Paradinas[a], Muriel Lissardy[c], Benoit Liquet[a,b]

[a] *CNRS/Univ Pau & Pays Adour, Laboratoire de Mathématiques et de leurs Applications de Pau - Fédération MIRA, UMR 5142, 64600 Anglet, France*
[b] *ARC Centre of Excellence for Mathematical and Statistical Frontiers at School of Mathematical Science, Queensland University of Technology, Brisbane, Australia*
[c] *Ifremer, LITTORAL, F-64600 Anglet, France*
[d] *Université de Toulon, Aix Marseille Université, CNRS, IRD, Mediterranean Institute of Oceanography (MIO), La Garde, France*
[e] *Univ. Pau & Pays Adour E2S UPPA, Chaire HPC Waves, Laboratoire des Sciences de l'Ingénieur Appliquées à la Mécanique et au Génie Electrique Fédération IPRA, EA4581, Anglet, France*

Corresponding author : Claire Kermorvant
email : claire.kermorvant@univ-pau.fr
ORCID ID : 0000-0002-1972-8937

Abstract:

Climate fluctuations affect a wide range of environmental factors that may impact fish populations with various response mechanisms. For a major part of world fisheries stocks, only abundance time-series are available. Relations between abundance of these species and ocean variables, including long term trends and patterns of seasonal change, remain sparsely documented. The main aim of our work is to determine to what extent effects of inter-annual and seasonal changes in environmental factors can be identified and quantified on a selected time-series of abundance data-set: the striped red mullet population within the Bay of Biscay. 8 Landings per unit of effort (LPUE) for striped red mullet data are compared with environmental covariates extracted from the Copernicus web database. Our strategy is to decompose the patterns of change in fish populations into long-term and seasonal components and to analyse the possible dependency of both components on environmental factors. The overall tendencies are a decrease of the long-term component and a modification of the seasonality, with additional spatial variability. The observed tendencies and seasonal changes are discussed against the spatio-temporal patterns of change in environmental factors. High spatial heterogeneity within the Bay of Biscay was found, both for striped red mullet long-term trends and seasonal changes. Most inter-annual and seasonal changes in striped red mullet abundance can be related to environmental factors. In addition to the well-known annual fluctuation, most coastal sites revealed a bi-annual seasonality possibly related to the recruitment process.

Keywords:

Bay of Biscay; Climate change; Environmental modelling; Fisheries indicators; *Mullus surmuletus*; Time-series decomposition.

1. Introduction

The fluctuations of ocean variables are a primary driver for fish populations (García-Barón et al., 2020). This environmental control has taken on particular importance in the context of global climate change, which affects numerous oceanic factors that may impact marine fauna (Brander, 2010). Due to the complexity of the mechanisms involved and the interactions between space- and time -varying driving factors, understanding the effect of climate change on these populations may prove to be tricky (Rijnsdorp et al., 2009). The effects of climate change on environmental factors, such as modifications of the water cycle, are expected to differ among geographic areas (IPCC, 2007), both at global and regional scales. For instance, river runoff and precipitation are expected to increase/decrease in northern/southern Europe, respectively (Frei et al., 2006). Likewise, ocean water properties are exposed to global change-induced modifications, such as the significant increase in salinity, which was observed during the three last decades in the northern part of the Atlantic ocean (Stott et al., 2008).

Several effects of environmental changes due to global warming on fish populations have already been reported (Both et al., 2006; Free et al., 2019). The review of Rijnsdorp et al. (2009) highlights that these changes may result in four response mechanisms. Firstly, changes in environmental parameters can induce a physiological response (Cohen et al., 2018). Secondly, modifications in environment may induce a behavioural response, such as moving into new suitable areas. The third type of response may be through population dynamics (i.e. changes in the balance between rates of mortality, growth, and reproduction in combination with dispersal) which could result in the establishment of new populations in new areas, in the abandonment of traditional sites or in a regime shift, with significantly higher or lower abundance than in other historical periods. Finally, a fourth response to environmental changes may be changes at ecosystem level (i.e. in productivity and/or trophic interactions). It should be emphasized that, even if this is expected to take on worrying proportions in the context of global change and increased fishing pressure, the characterization of the response of fish populations to the fluctuations of ocean variables is already a major challenge for ocean ecology scientists.

From an ecological perspective, the study of the relationships between environmental factors and populations is generally carried out using three main categories of models (Melo-Merino et al., 2020): mechanistics models (Kearney and Porter, 2009), process-oriented models (Peterson et al., 2015) and correlative models (Huntley et al., 1995; Araujo and Guisan, 2006; Franklin et al., 2009; Box, 2012). A direct application of such modelling strategies in a marine ecosystem remains very challenging. A major limitation is that most environmental data layers are not know in the entire three-dimensional ocean (Assis et al., 2016). Another difficulty arises from the lack of knowledge on dynamics and behaviour for most species (Bentlage et al., 2013). For fisheries stock assessment, the International Council for Exploration of the Sea (ICES) divide fish stocks into 6 categories. Categories 2 to 6 belong to data-limited categories (Lart, 2019). The majority of the world's fisheries, by number, are classified in these categories (Costello et al., 2012; Dowling et al., 2019). A stock can be considered as data-limited for various reasons, including a lack or a limited amount of reliable data, incomplete surveys and/or poor sampling leading to uncertainties about the biology of the species (Le Quesne et al., 2013). For ICES categories 5 and 6, abundance is only indirectly assess through selected proxies, and ecology and behaviours are almost unknown. In such a context of data limitation which inhibits comprehensive understanding of fish behaviour, the alternative approach followed here is first to use a non-causal statistical approach, i.e. to identify and quantify dependencies between the level of interest and the available environmental covariates without any *a priori* knowledge of the driving mechanisms, and then to infer *a posteriori* causal relationships by combining statistical results and expert knowledge.

Apart from the data quality issue, the extraction of entangled trends and patterns in time-series data remains a major challenge for data processing science. A widely used approach is to split the time series into several components, possibly selected from an *a priori* knowledge of the driving factors (Hyndman and Athanasopoulos, 2018). A number of decomposition methods are available in literature in relation to the very variable nature of the data-sets, including for instance intermittency, shortness, instationarity, non-linear response to driving factors (Huang et al., 1998). Standard data processing books, see e.g. Brockwell et al. (1991), or more recently Shumway and Stoffer (2017), review and detail a large panel of decomposition methods, the latter with examples of application under R software. Under global change effect, the data from

the Bay of Biscay, situated at mid-latitude, may be expected to respond to climate factors affected by both global long term trend and annual seasonal fluctuations. A helpful time-series decomposition can be therefore be based on the extraction of long term trend and seasonality from the time-series, with an additional residual (Ferguson et al., 2008). Such a time-series decomposition into trend, seasonal and residual components is still rarely used in fish ecology (Broekhuizen and McKenzie, 1995; Beare and McKenzie, 1999). Among the rather rare attempts, Plaza et al. (2018) used time-series decomposition as a method of data filtering, to identify contrasts between data features and technical fisheries literature, and Hsieh et al. (2009) analysed links between larval anchovy data and environmental variables. More generally, time-series decomposition methods, while widely used in data processing, are not familiar to ecologists (Hsieh et al., 2009).

The present study is, to our knowledge, the first assessment of the effect of changes in environmental factors on data-limited fish populations using the time-series decomposition method. The target species is the striped red mullet, *Mullus surmuletus Linnaeus*, 1758. The striped red mullet is distributed in the Mediterranean Sea and along the Eastern Atlantic coasts, from the English Channel to the northern part of West Africa (Labropoulou et al., 1997). At a large scale (Atlantic ocean), northerly migration of striped red mullet during a phase with demonstrated temperature increases due to climate change has already been demonstrated (McCarty et al., 2001; Hulme, 2002; Beare et al., 2005). Striped red mullet abundance increases in the English Channel (Vaz et al., 2004) and the North Sea. Eastern English Channel and the Bay of Biscay are two main areas of catches of striped red mullet in the Atlantic Ocean (Mahe et al., 2014). Individuals in the Bay of Biscay belong to the sub-population individualized in Western Europe by ICES. It extends from the Celtic sea to the waters bordering the Iberian Peninsula with a significant presence in the Bay of Biscay. It is a predominantly benthic and gregarious species living in small groups of up to a dozen individuals. It can also be solitary or live just in pairs. Young fishes live in lower salinity coastal areas while adults have a more offshore distribution (Oskarsson et al., 2019). Pajuelo et al. (1997) find young striped red mullet between 10 and 60 m deep in Canaries Islands while (Reñones et al., 1995) report values between 30 and 90m in Majorcan waters. The striped red mullet has an inter-depth migration because of its reproduction (Kousteni et al., 2019). The recruitment occurs in shallow habitat (García-Rubies and Macpherson, 1995), spawns in deep habitats and continue to disperse into deep water after reproduction (Machias and Labropoulou, 2002). On average, striped red mullet abundance is highest in surface waters down to 100 m depth (easily observable from 0 to 30 m) (Mahé et al., 2005), but large specimens have been observed below 300 m depth. In the north Atlantic, mature striped red mullet depths is between 100 and 200 m on average (Leaute et al., 2018). Several factor may intervene in the abundance of the striped red mullet. Benthic habitat composition (Ajemian et al., 2016) or substrate type (Lombarte et al., 2000; Mahé et al., 2005) are important. As for all other species, other factors can affect striped red mullet and may have an important impact on its abundance. In particular, population may be affected by trophic web parameters, such availability of preys and abundance of predators, or factors related to natural mortality such as diseases and parasites. Recent study reports life-history traits of the striped red mullet in Mediterranean (Kousteni et al., 2019). Longevity of striped red mullet is estimated at 11.75 years and the length at 50% of maturity is 153.3 mm for females and 139.2 mm for males.

Following the ICES classification categories (ICES, 2012), Bay of Biscay sub-population is currently in data-limited stocks (DLS) category 5: it is a stock for which only landing data are available, as described above. From a fish population perspective, the Bay of Biscay remains a limited area with a total surface aire of approximately 223 000 km^2. No substantial scientific literature is available to qualify the striped red mullet stock status within the Bay of Biscay and its relationship with ocean variables, whether in the past, at present or in the global change context.

The aim of the present paper is to determine whether modifications of oceanic environmental factors, such as changes in long term or seasonal trends, have an impact on the striped red mullet population within the Bay of Biscay. The analysis will be based on selected professional LPUE (Landing Per Unit Effort) as a proxy of striped red mullet stock abundance in the Bay of Biscay, as suggested by Caill-Milly et al. (2019). Time-series decomposition was first applied on striped red mullet abundance to achieve a rough understanding of the population dynamics through space and time. Secondly, the analysis was dedicated to the identification and quantification of possible links between trends and seasonal fluctuations of both striped red mullet

abundance and environmental covariates. The results and methodology were then discussed, keeping in mind the challenge of the limited time span of the available time-series on for striped red mullet index of abundance.

2. Methodology

2.1. Database

2.1.1. Fishery data

The fishery database used for the present paper (Kermorvant et al., 2020) was provided by the SACROIS (SACROIS) algorithm developed by Ifremer. SACROIS is a cross validation tool for fisheries statistics, in response to Article 145 of the EU regulation (EC Reg. 404/2011). SACROIS algorithm cross-checks information from fishing forms, fishing fleet registers, logbooks, sales notes, VMS data and the scientific census of fishing activity calendars (Mateo et al., 2016). We have selected this database because we considered that it is the most complete available database regarding production and fishing effort data for the French fleet operating in the Bay of Biscay. The SACROIS data are spatially aggregated by ICES rectangles assembled monthly. ICES rectangles extend about 0.5 and 1 degree in longitude and latitude, respectively, with an area of approximately 30 nautical squared miles. The present study was based on a set of six coastal ICES rectangles selected because they were sufficiently documented to allow time and time-frequency analysis (see Figure 1A). These selected rectangles do not integrate the full ecological niche of striped red mullet in the Bay of Biscay, but were each inside the niche and contain sufficient information to be considered as representative of the Bay of Biscay striped red mullet population ICES (2019). LPUE was provided for a given gear, gear mesh, day and ICES statistical rectangle. Specific vessels, i.e. small trawl vessels (7.9–15.8 m) with a gear mesh of 70–79 mm, were selected in the SACROIS database following the criteria of Caill-Milly et al. (2019) for striped red mullet. The time series of the selected mean trawlers LPUE was available from 2005 to 2018. LPUE is not a direct estimator of abundance. However, applying, (i), a filtering on vessel and gear characteristics and, (ii), a selection of a period without significant changes in regulation [see Caill-Milly et al. (2019)], we considered that the selected daily LPUE was a relevant proxy for striped red mullet abundance. In fisheries-dependent data, bias can be introduced to abundance estimates when sampling was not randomized (Potts and Rose, 2018). Striped red mullet is of high commercial interest but is not specifically targeted by trawlers in the Bay of Biscay (it is a part of set of sought-after demersal species). Therefore, even if the sampling scheme was not randomized, it was not directed. Futhermore, the International Council For the Exploration of the Sea (ICES) identified striped red mullet LPUE as a potential abundance index for this stock (Oskarsson et al., 2019; ICES, 2020). Note that, as the present analysis requires continuous time-resolved database, other available sources of data at lower sampling rates (such the EVHOE campaign in the Bay of Biscay and Celtic Sea) were not considered.

2.1.2. Environmental data

Environmental data was extracted from the Copernicus portal (https://www.copernicus.eu). Values for surface temperature (in degree Celcius), surface salinity (in grams per liter), phytoplankton concentration (in $mmolC/m^3$), chlorophyll concentration (in mg/m^3, and chemicals (Silicate (Si), Phosphate (PO_4^{3-}), Ammonium (NH_4^+), Nitrate (NO_{3-}) and Dissolved Oxygen ($mmol/m^3$) were selected from 2005 to 2018 within the Bay of Biscay. For surface temperature and surface salinity, main statistical values (table 1) were computed for each environmental variable by ICES rectangle. For phytoplankton concentration, chlorophyll concentration, and chemicals, a first statistical study showed a high correlation. A principal component analysis (PCA - available in appendix) was therefore used to reduce the number of variables. Based on the eigenvalues of the three first axes, three new variables were produced, namely PC1, PC2 and PC3. PC1 is driven by Si, PO_4^{3-} and NH_4^+ and explain 57.2% of variability, PC2 by phytoplankton, net primary production and NO_{3-} and explain 18.6% of variability. PC3 by Dissolved Oxygen and explain 10.2% of variability.

Tab.1 here

2.2. Data processing

2.2.1. LPUE time-series decomposition

Our strategy to analyse the spatio-temporal dynamics of striped red mullet abundance was to assume an additive decomposition of the LPUE in terms of a Long Term Trend (LTT), a Seasonal Trend (ST) and a residual R. LTT aimed to describe the interannual changes in LPUE while ST was dedicated to characterizing the amplitude of the seasonal fluctuations. LPUE time-series exhibited a very high variance and needed to be log transformed to be modelled at a given time t (in months from January 2005 to December 2018) and location r, Y_{rt} being here below the value of $log(LPUE_{rt})$, the decomposition was written:

$$Y_{rt} = LTT_{rt} + ST_{rt} + R_{rt}. \tag{1}$$

2.2.2. Long Term Trends

For each rectangle r, a moving median ($MM(Y_{rt})$) over a 48-month window was applied to remove intra-annual or seasonal effects and then investigate appropriate model for estimating the LTT. We proposed to investigate the Long Term Trends applying a smoothing function to time:

$$MM(Y_{rt}) = \alpha_r + f_r(t) + \epsilon_{rt}, \tag{2}$$

where ϵ_{rt} follows a normal distribution $\mathcal{N}(0, \sigma^2)$. The smooth function of each rectangle $f_r(\cdot)$ is defined using spline bases [see Wood (2017)]. In practice we used generalized additive model (GAM) through the `mgcv` R package provided by Wood (2017). Note that an intercept α_r by rectangle was required due to some optimization constraints used in `mgcv` (see Chapter 5 and 7 of Wood (2017)).

The fitted model (2) provided a smooth estimation of the time-dependent inter-annual trend for each rectangle: $\widehat{LTT_{rt}} = \widehat{\alpha}_r + \widehat{f_r(t)}$.

2.2.3. Seasonal Trends

The seasonal component was obtained by removing the estimated trends from the initial $log(LPUE)$ data:

$$ST_{rt} = Y_{rt} - \widehat{LTT}_{rt}.$$

The subsequent analysis is twofold:

- The first bulk Seasonal Trend model in each rectangle was obtained from dynamic harmonic regression Young et al. (1999):

$$ST_{rt} = \sum_{j=1}^{K_r} \{\alpha_{0,r} cos(\omega_j t) + \alpha_{1,r} sin(\omega_j t)\} + \epsilon_{rt} \tag{3}$$

  where $\omega_j = \frac{2\pi}{m} j$ are the harmonic frequencies associated with the seasonality in the series, m being the annual number of months, i.e. 12. $\epsilon_{rt} \sim \mathcal{N}(0, \sigma_r^2)$. Depending on the selected rectangle, a range of harmonics ($2 < K_r < 6$) were tested to provide the best model based on AIC comparisons (Sakamoto et al., 1986). This first bulk Seasonal Trend model in each rectangle provided an overview of the LPUE seasonality.

- Further insight on LPUE spatio-temporal dynamics was provided by a time-frequency analysis of the seasonal component. A discrete Fourier analysis (Bloomfield, 2004) was performed on the seasonal component for each ICES rectangle to provide the spectral density (i) over the complete time-series and (ii) over a moving 48-month window for time-resolved analysis. From the latter analysis, the amplitude of seasonal fluctuations associated with annual (12 months) and biannual (6 months) periods were extracted, named $ST^{12}_{LPUE,rt}$ and $ST^{6}_{LPUE,rt}$, respectively:

$$ST^n_{LPUE,rt} = \sqrt{\int_{f_1}^{f_2} SD(u)du} \tag{4}$$

where $SD(\cdot)$ is the spectral density (Stoica et al., 2005), $n = 6$ or 12 for biannual and annual fluctuations, respectively and f_1 and f_2 are the frequency boundaries taken at 5 and 8, and 9 and 16 for the biannual and annual fluctuations.

2.3. Dependency on environmental variables

2.3.1. Long Term Trends

Models for Long Term Trends were defined for environmental covariates time-series similarly as done for LPUE (see Eq. 2). Links between estimated long term trends of LPUE (noted $\widehat{LTT}_{LPUE}$) and various environmental covariates were first tested using an uni-variate linear model. Five relevant environmental variables were then selected for the multivariate linear model: the fitted trend of median water salinity $\widehat{LTT}_{MS}$, the fitted trend of median surface temperature $\widehat{LTT}_{MT}$, and the fitted trends of PC1, PC2 and PC3 variables $\widehat{LTT}_{PC1}$, $\widehat{LTT}_{PC2}$ and $\widehat{LTT}_{PC3}$, respectively. For each rectangle, we modeled:

$$\widehat{LTT}_{LPUE,t} = \beta_0 + \beta_1\widehat{LTT}_{MT,t} + \beta_2\widehat{LTT}_{MS,t} + \beta_3\widehat{LTT}_{PC1,t} + \beta_4\widehat{LTT}_{PC2,t} + \beta_5\widehat{LTT}_{PC3,t} + \epsilon_t, \tag{5}$$

where $\epsilon_t \sim \mathcal{N}(0, \sigma^2)$.

2.3.2. Seasonality

The seasonal component of environmental covariates was processed by time-frequency analysis similarly to the LPUE data. For each variable and each rectangle, the annual and biannual amplitudes of seasonal fluctuations were obtained from the time-resolved spectral density over a 48-month moving window.

A linear model was built by rectangle to test the relationship between the annual and biannual amplitudes of seasonal fluctuations of LPUE and environmental covariates data:

$$ST^n_{LPUE,rt} = \gamma_0 + \gamma_1 ST^n_{MT,t} + \gamma_2 ST^n_{MS,t} + \gamma_3 ST^n_{PC1,t} + \gamma_4 ST^n_{PC2,t} + \gamma_5 ST^n_{PC3,t} + \epsilon_t. \tag{6}$$

where $n = 6$ and 12 for biannual and annual fluctuations and ϵ_t follows $\mathcal{N}(0, \sigma^2)$.

2.3.3. Models performance

Some parameters were selected for each linear model created for LTT and ST. Firstly, estimates of the coefficient of the linear regression and associated p-value were recorded. Estimates is the mean change in the LTT or ST for one unit of change in the covariate. A low p-value (e.g. <0.05) means changes in the LTT or ST value are related to changes in the covariate. Secondly, the global R^2 and relative importance per covariate were calculated. The model global R^2 indicates the proportion of variance of LTT or ST explained by the created model. Relative importance of covariate enables us to determine the share of variability accountable for each environmental covariate. In other words, relative importance of covariate is the proportionate contribution each covariates makes to global R^2. Relative importance of covariates was calculated with the `relimpo` package of R software (Grömping et al., 2006). The used metric is "lmg", which provides a decomposition of the model explained variance (Grömping et al., 2006).

3. Results

3.1. LPUE time-series decomposition

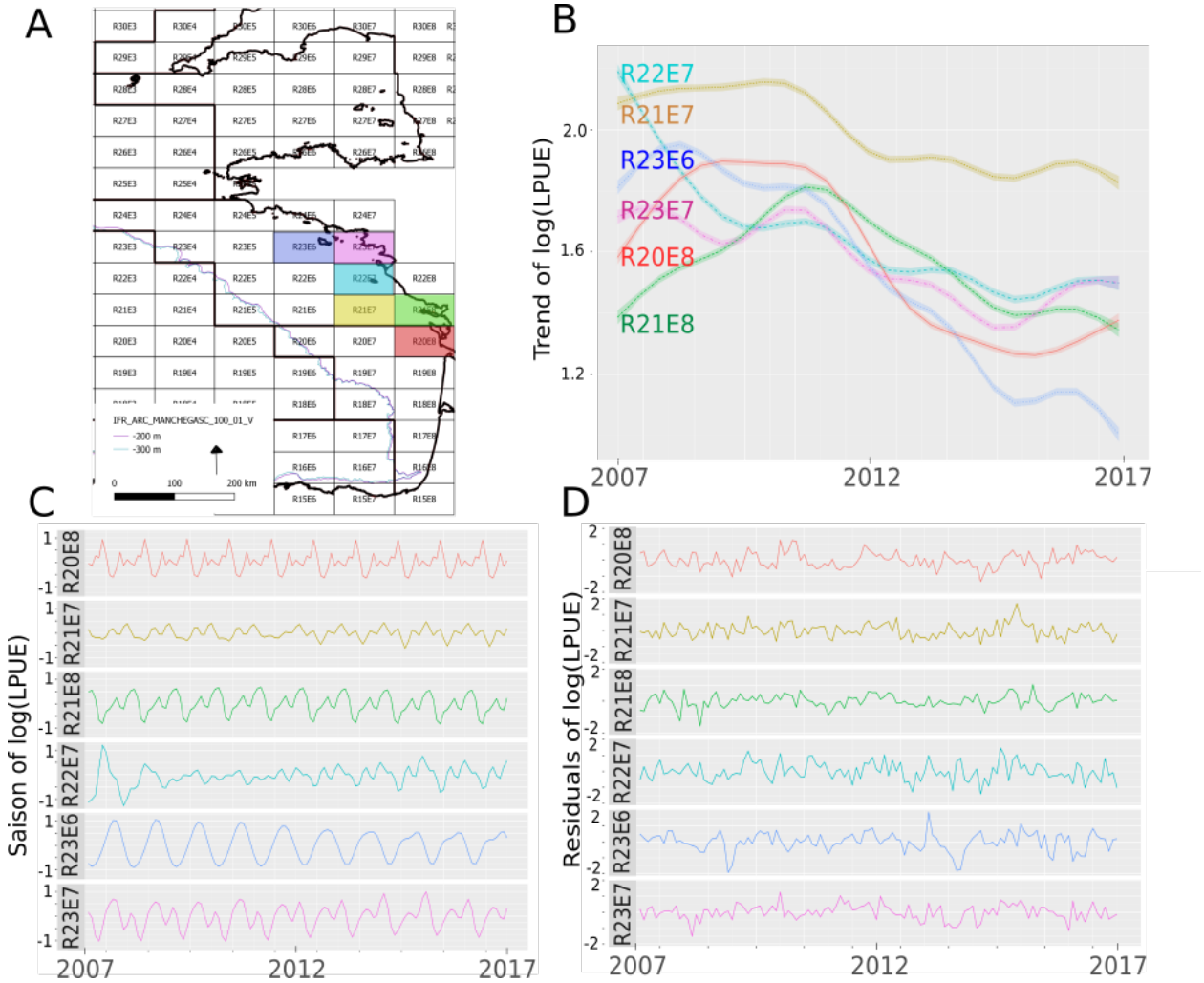

Figure 1: Time-series decomposition in striped red mullet abundance. A: Map of studied rectangles. B, C and D: Long Term Trend (LTT) and associated GAM error, Seasonal Trend (ST) and Residual (R) of $log(LPUE)$ by ICES statistical rectangle, respectively.

Figure 1A presents the locations of the ICES rectangles in this study. Data were recorded from 01/01/2005 to 12/31/2018. Due to moving average processing, the two first and the two last years of data were deleted. Data are so presented from 01/01/2007 to 12/31/2016. The first observation in Figure 1B was an overall decreasing of $\widehat{LTT}$ of $log(LPUE)$ during time, with an average value of approximately 20 % between 2006 and 2017. To go further we used a linear model by rectangle to assess the ability of $\widehat{LTT}$ to explain initial $log(LPUE)$. $\widehat{LTT}$ variable is significant (p-value < 0.01) in almost all linear models to explain log(LPUE) data, but not for rectangles R23R7 and R22E7. A finer analysis of Figure 1B revealed a significant spatial variability in time evolution of striped red mullet abundance with three main periods: 2006-2010, 2010-2014 and 2014-2017. First, during the 2006-2010 period, R23E7, R23E6 and R21E7 showed weakly fluctuating values, R20E8 and R21R8, situated at the southeast of the study area, showed a significant increase and

R22E7 showed a clear decreasing trend. The second and third periods, respectively 2010-2014 and 2014-2017, showed more spatial consistency. The former period was characterized by a global decrease for all zones while the latter period showed overall more stable values.

Seasonal patterns computed using Equation 3 also highlighted spatial variability, see Figure 1C. Significant intra-annual fluctuations were observed for most ICES rectangles. A striking observation was the time and space variability of these seasonal fluctuations. Such variability in the frequency domain calls for more detailed spectral analysis which will be presented in Section 3.3. The only zone clearly dominated by uni-modal distribution is R23E6, i.e. the most north-westerly rectangle studied. Other rectangles showed additional periodic bi-modal or higher frequencies fluctuations. The time-change was also spatially variable, with a quite steady seasonal shape for R20E8, R21E8, R23E6 and R23E7 rectangles and more visible change for R21E7 and R22E7. For this latter area, the seasonal signal nearly drops to zero between 2009 and 2011 before regaining values similar to other zones.

Figure 1D shows decomposition residuals. For all sites, the residuals did not exhibit any discernible pattern. This confirmed that the selected additive decomposition had extracted most of the relevant information in the striped red mullet abundance time-series.

3.2. Long term effects

Figure 2 depicted the comparison between $\widehat{LTT}$s for striped red mullet abundance and selected environmental covariates. Results were first presented in qualitative terms, while a more quantitative analysis is provided hereafter by the linear model. $\widehat{LTT}$ for $log(LPUE)$ was described and compared in the previous section (see Figure 1B). $\widehat{LTT}$ for environmental covariates generally shown a strong spatial variability. The surface salinity (MS) was lower for coastal rectangles R23E7, R21E8 and R20E8 due to the continental freshwater inputs, in particular by the Garonne and Charente rivers. For most rectangles, the overall trend was a slight decrease of salinity affected by a rise during the 2010-2012 period. The surface temperature (MT) shown the expected meridional variation (higher temperature in the south) and an overall increase for all rectangles. For the northern areas (R23E6, R23E7 and R22E7), the temperature tended to vary in the opposite way to the salinity: low temperatures were associated with high salinity during the 2009-2012 period while rising temperatures were associated with lowering salinity after 2012. This trend was less marked for the southern rectangles. The PCA-reduced environmental variables were generally well connected in space. $\widehat{LTT}$ for PC1, PC2 and PC3 were maximal in coastal regions R21E8, R20E8 and R22E7 and decreased offshore in R21E7 and R23E6. The only exception was the R23E7 coastal rectangle for which PC1 was maximal while PC2 and PC3 was minimal. Chnages over time for PC1 were generally very weak. Stronger dynamics were observed for PC2, for which low values were associated with low temperatures and high salinity events and, inversely, to rise after 2012 when salinity/temperature are generally decreasing/increasing. For PC3, the signal was nearly stable for R20E8 and R21E7 and mainly decreasing for R21E8, R22E7 and R23E6, without any straightforward relation with other environmental covariates. For R23E7, PC3 followed PC2 trends, with a strong link with surface temperature.

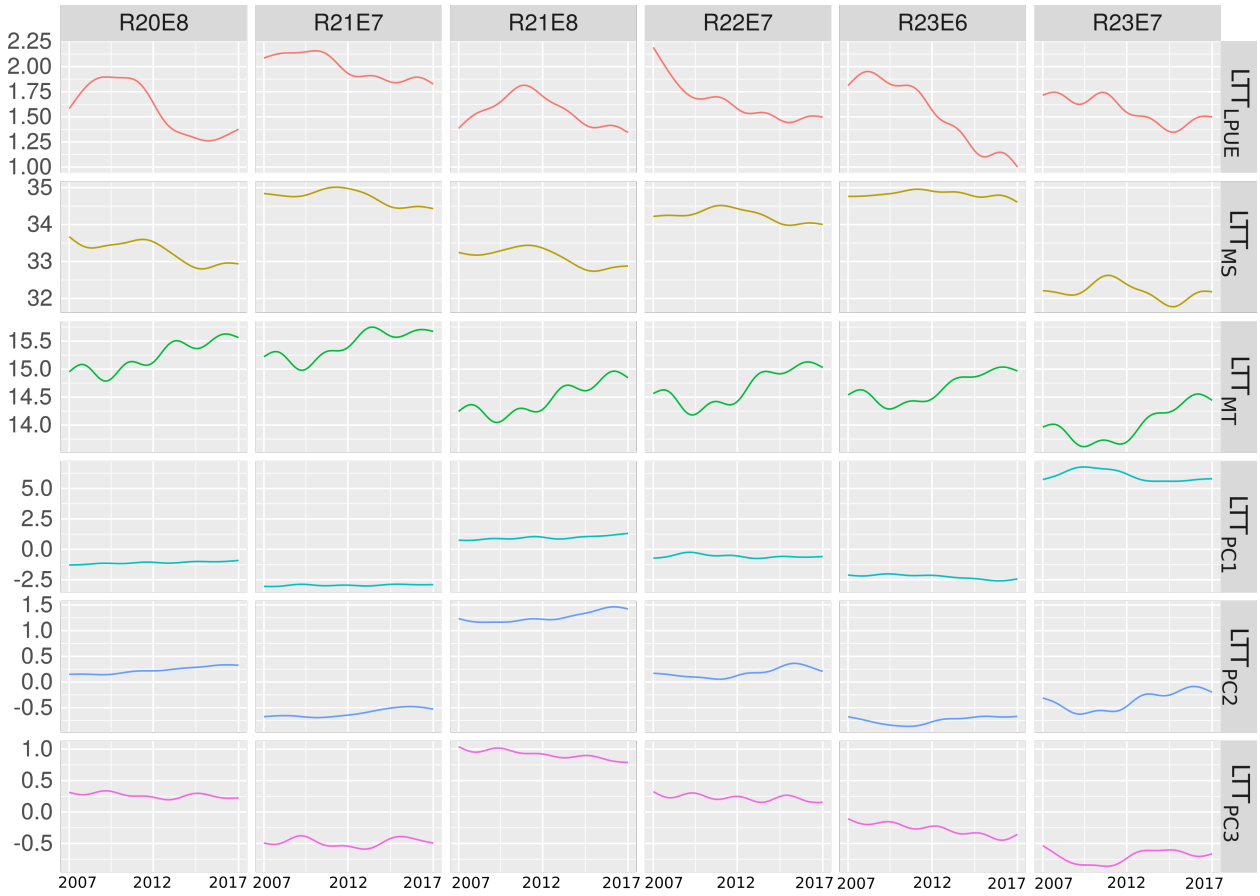

Figure 2: Long Term Trends (LTT) for striped red mullet abundance and environmental covariates for all studied ICES rectangles. LPUE is landing per unit of effort, expressed in monthly mean of daily kg by rectangle, MS is salinity in grams per liter and MT is temperature in degrees Celsius.

The linear model presented in Equation (5) was used to assess quantitatively the relationships between $\widehat{LTT}$ for striped red mullet abundance and environmental variables. The results were summarized in Table 2. The first observation was that all R^2 values were above 0.8 (excepting R22E7 which shows $R^2 = 0.65$), meaning that trends in environmental variables were able to explain at least 80% of trends in striped red mullet abundance. Note that these R2 values were not directly related to the raw data and they had to be interpreted on the explained variance of the extracted long term trends $\widehat{LLT}$ of the LPUE obtained from 2 by the long term trends of environmental variables. Our main goal was to investigate and highlight the importance of variables to explain striped red mullet LPUE. Another observation was that striped red mullet abundances were predominantly positively affected by salinity for five out of six rectangles. For the coastal rectangles R20E8, R21E08 and R23E7, striped red mullet abundance could be linked to continental freshwater inputs. The role of temperature was mainly significant in the two northern zones R23E6 and R23E7, with striped red mullet abundance favored by higher temperature. PC1 generally played a weak role except in the most northwestern zone R23E6/R23E7. PC2 was negatively correlated to abundance in all rectangles except the most southeastern ones R21E8 and R20E8. PC3 displayed stronger positive correlations only for the northern zones R23E6, R23E7 and R22E7.

Tab. 2 here

3.3. Seasonality

Figure 1 revealed the spatial and temporal variability of the LPUE seasonal component using a bulk harmonic approach. Further insight was provided by the spectral density computed, for each rectangle, over the complete time series, see Figure 3. The spatial discrimination was straightforward: coastal rectangles R20E8, R21E8 and R23E7 were the only ones to show both biannual (6-month period) and annual (12-month period) fluctuations. The offshore rectangles R23E6 and R21E7 shown a single annual seasonality, although less marked for R21E7 than for the northwestern R23E6. The remaining rectangle R22E7 had a noisy spectral density. This lack of consistency for the spectrum was related to the fluctuations of seasonality, both in amplitude and period, during the acquisition period revealed in Figure 1.

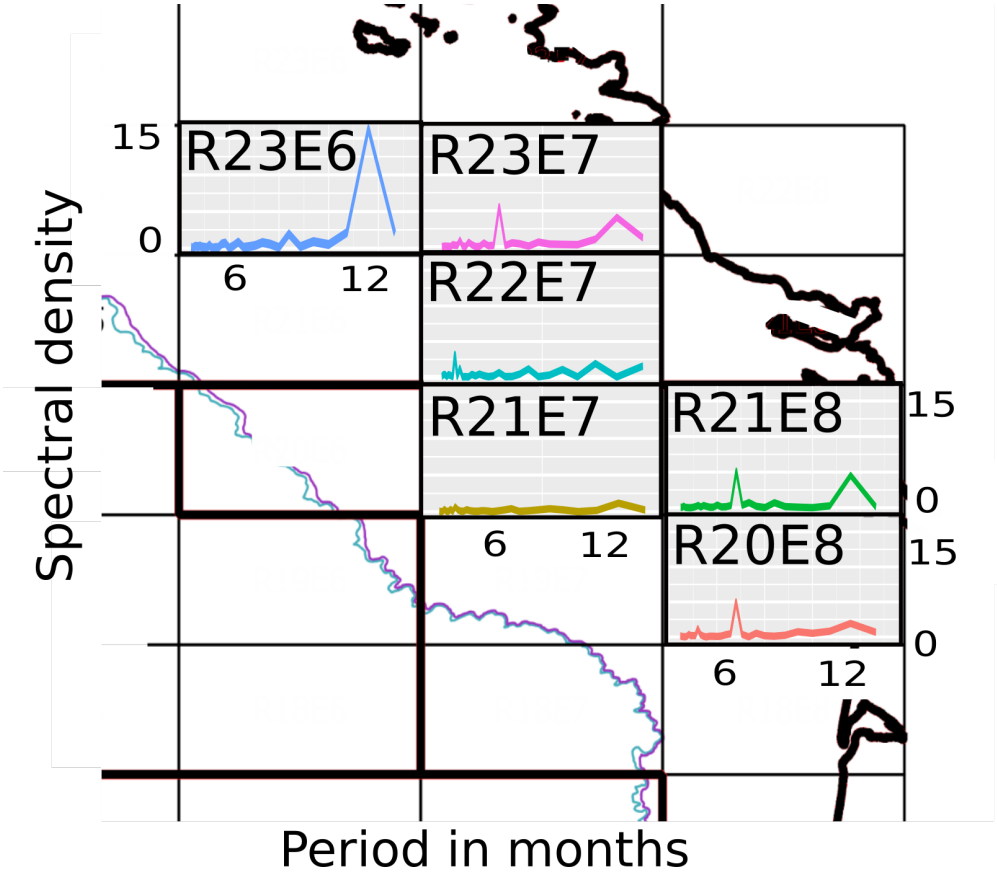

Figure 3: Spectral density of log(LPUE) for each ICES rectangle over the complete time series.

Based on the time-resolved spectral density over a 48-month moving window, the amplitudes of annual and biannual seasonal fluctuations (Eq. 4) were computed in each rectangle for $log(LPUE)$ and environmental covariates. An illustration of the results for rectangle R23E7 is presented in Figure 4. The spectral density computed over the complete time-series (Figure 4A) revealed that the biannual (6-month) peak observed in $log(LPUE)$ can not be connected to any similar seasonal component in the selected set of environmental covariates while the annual (12-month) peak in $log(LPUE)$ surely had a link with the annual peak observed in all selected environmental covariates.

The time-resolved spectral analysis of biannual and annual fluctuations over a 48-month moving window was shown in Figures 4B and C, respectively. Biannual seasonality of abundance was variable but the level observed between the start and the end of the studied period did not show any trend and was qualitatively

uncorrelated to environmental covariates. Annual seasonality for $log(LPUE)$ shown slightly greater change over time, with minimal values reached between 2009 and 2013. Annual seasonality for environmental covariates also revealed more consistent patterns over time.

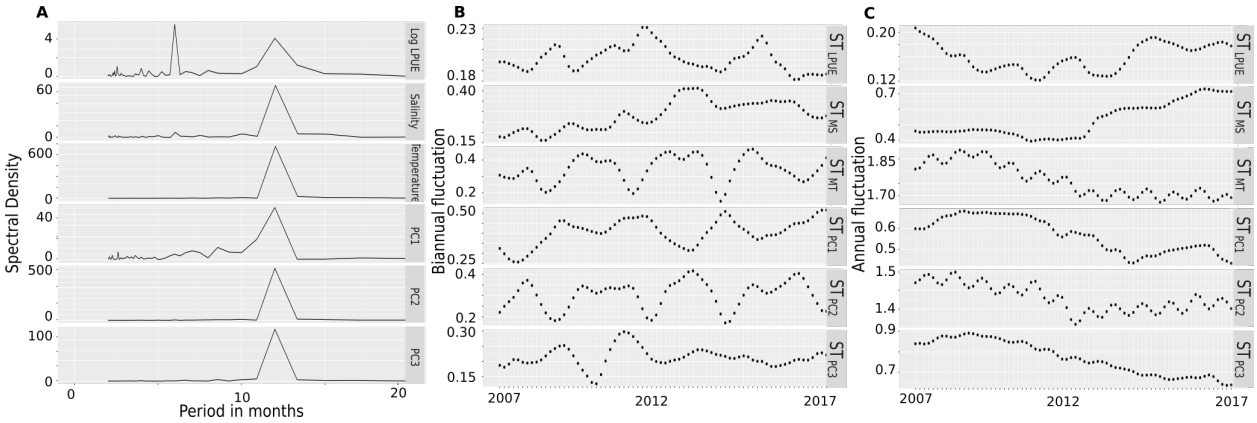

Figure 4: Time-frequency analysis for rectangle R23E7. A: spectral density for $log(LPUE)$ and environmental covariates over the full time-series. B and C: time-resolved magnitude of seasonal fluctuations over a 48-month moving window for biannual and annual components, respectively, for $log(LPUE)$ and environmental covariates.

The multivariate linear model presented in Equation 6 was used to evaluate comprehensively the relationship between abundance and covariate seasonality. Complete results were shown in Table 3.
Figure 3 previously demonstrated that the annual seasonality of striped red mullet abundance was well developed for rectangles R21E8, R23E6 and R23E7 and to a lesser extent for rectangles R20E8 and R21E7. Table 3 further indicates that the dependency of abundance seasonality on environmental covariates seasonality was not systematic and not spatially uniform. PC1 annual seasonality appeared to affect abundance annual seasonality in rectangles R20E8 and R23E6, with negative and positive correlations, respectively. R20E8 was furthermore connected to the annual fluctuations of salinity and temperature: abundance seasonality was favored by strong temperature and weak salinity fluctuations. R21E7 and R21E8 were connected to salinity and temperature annual fluctuations, respectively, while R23E7 annual seasonality did not show any significant relation with environmental parameters.

Biannual seasonality of $log(LPUE)$ was well established in the three coastal rectangles R20E8, R21E8 and R23E7 (Fig.3). For the latter rectangle, the biannual seasonality was not related to environmental covariates seasonality, similarly as for annual seasonality. PC1 biannual seasonality was observed to affect both R20E8 and R21E8, while salinity biannual seasonality only affected R20E8.

Tab. 3 here

4. Discussion

The aims of the present study were (i) to assess long-term and seasonal changes in striped red mullet abundance in the Bay of Biscay, and (ii) to identify the possible relationships between changes in abundance and environmental factors. This study was carried out on the basis of an indicator of abundance, which was the sole information available for striped red mullet natural fish populations within the Bay of Biscay. As no appropriate methodology to tackle this problematic with these data already existed in literature, we had to develop a new one. Thus, the main aim of this study was not to present a new methodology, but to better understand the effects of the environment on striped red mullet abundance. Here, we will discuss results and compare them with other studies, but some conclusion will remains hypothtical due to a very poor documentation in literature on the ecology of striped red mullet.

Long term trends were inferred from the abundance data using a moving average with a smoothing function. The resulting trends were clearly non-linear, thus ruling the use of linear approaches (see Hess (2001); Lentka and Smulko (2019) for trends detection). Seasonal components were processed using time-frequency analysis with moving-window spectral computations, which highlighted the strong fluctuations of the abundance seasonality both in space and time. Other tools for time-frequency analysis could have been used here such as the wavelet analysis (Huang et al., 1998). It is important to note that time-frequency analysis is strongly constrained by the need to have continuous and long enough time-series.

The selected environmental variables also shown non-linear long term trends. These observations result from the complex interactions between a large number of processes affected by fluctuations over wide ranges of space and time scales which were outside of the scope of the present study. However, from a data-processing perspective, it is again worth noting to note that, in our study zone, coupled ocean-atmosphere systems such as the North-Atlantic Oscillation (NAO) (Hurrell, 1995) or other fluctuating large scale climate patterns (Castelle et al., 2017) provided additional variability to the global change track. For instance, the overall warming of the ocean surface observed from the present analysis of Copernicus database, well documented in the literature (Peck and Pinnegar, 2019; deCastro et al., 2009; Koutsikopoulos et al., 1998; Planque et al., 2003), combines with inter- and intra-annual oscillations and spatial variability. Similarly, salinity and PCA-reduced environmental variables showed strong time and space variability. Such results could be related with climate-driven patterns (Roessig et al., 2004) of atmosphere properties, precipitation, land runoff, river discharge, etc. This reinforces the relevance of the present approach to determine trends and relationships between fish populations and environmental factors.

the study of long term trends in striped red mullet abundance shown a high spatial heterogeneity within the Bay of Biscay even on a relatively small scale. The dominant trend was a decrease in striped red mullet abundance. This decrease varied among the studied ICES spatial rectangles. But, for almost all rectangles, we could link 80% of this trend variance to environmental covariates trends. The dependency on environmental covariates was also spatially variable. In coastal rectangles, long term trends of abundance can had a slight positive link with surface salinity trends. While for more off-shore rectangles, striped red mullet abundance increased along with salinity. Striped red mullet salinity preference was detected to be between 35.1 and 35.6 grams per liter (Desbrosses, 1935). These values were for adults fishes at depths between 100 and 200 meters. One possible explanation for positive link in trends between striped red mullet abundance and salinity in coastal rectangles is that the striped red mullet is at the lower limit of its salinity ecological niche in coastal rectangles (see table 1). When salinity decreases in coastal zones, due to inland freshwater inputs, striped red mullet abundance decreases. More precise information about the striped red mullet ecological niche is needed to consolidate this hypothesis of a positive link between striped red mullet abundance trends and salinity in coastal zones.

In the southern Bay of Biscay, striped red mullet have already been detected as species with an affinity for warm temperatures (García-Rodríguez et al., 2011). In our study area, in the northern Bay of Biscay, mean sea surface temperature was around 14.5 degrees Celsius for the colder rectangles and 15 degrees Celsius for the warmer rectangles. We did not detect links between temperature trends and striped red mullet abundance except for the two coldest rectangles. In these two northern rectangles, abundance trends decreased when temperature trends decreased and conversely, which tends to confirm the observation of García-Rodríguez et al. (2011). For a similar species *M. barbatus* in Aegean Sea, abundance has been proved to be higher in warm bottom water (19^{o}C) than in colder waters (Maravelias et al., 2007). In addition, this species seems to avoid the cold bottom waters ($< 16^{o}$C) (Maravelias et al., 2007). An hypothesis to explain the freshness of the two northern rectangles is they are in a river freshwater inputs and up-welling zone. This hypothesis is favoured by the study of Puillat et al. (2006) demonstrating some events of up-welling-favourable winds exactly in the zone were we found the lowest temperature, and a positive link with striped red mullet abundance. In these rectangles, red-mullet is at the edge of its favoured life condition regarding temperature. When water temperature decreases, striped red mullet falls outside its life *preferendum* and abundance decreases.

Up-welling and river discharges also induce chemical transports or dissolution from sediments. In this study, we have attempted to find a relationship between striped red mullet abundance and chemical concentrations

in the sea water. As strong correlations were initially observed between different chemical species, we chose to perform a dimension reduction with PCA. But, interpretation of linear model estimates of PCA reduced dimensions can be delicate. Only the two southern rectangles do not shown a link with PCA reduced dimensions. For the four other rectangles, trends in striped red mullet abundance were linked to chemicals and primary production. The link was positive with PC3. As PC3 had a positive contribution of O_2 concentration, we can say striped red mullet abundances were positively linked to O_2 concentration. This result is consistent with studies highlighting an increase of capture probability of an other mullet species along with dissolved oxygen rate (Maes et al., 2007). In the four northern rectangles, trends in striped red mullet abundance were also positively linked with PC1. PC1 is built from a negative contribution of Si, PO_4^{3-} and NH_4^+, meaning that striped red mullet abundance was negatively linked to Si, PO_4^{3-} and NH_4^+ concentrations. The effect of chemicals, phytoplankton and net primary production rates on striped red mullet abundance were never investigated. Further investigations are required to confirm the present original observations.

The seasonal study revealed high variability of striped red mullet abundance seasonality within the Bay of Biscay. In the most off-shore rectangle, striped red mullet abundance shown well defined annual oscillations while in the most shoreward ICES rectangles, additional biannual oscillations were observed. In the two remaining ICES rectangles, no clear periodic pattern was observed. Multiple peaks per year when studying seasonality in fisheries stock abundance were already reported in the case of multiple species studies (Hsieh et al., 2009), but such a variability for a single species was not reported before, to the best of our knowledge. One peak in seasonality of annual abundance occured at intermediate depth. Following the literature on striped red mullet ecology, spawning commonly occurs in spring and early summer (May and June) (Desbrosses, 1935; N'Da and Déniel, 1993; Mahé et al., 2005; Leaute et al., 2018). Even if massive movement of spawners during reproduction has not been reported for striped red mullet, our best hypothesis regarding the annual seasonal peak in striped red mullet abundance may reflect movements during reproduction process. But, to our knowledge, it has to date never been statistically proven. We also modeled this one peak annual seasonal fluctuation of striped red mullet abundance along with similar environmental annual seasonal fluctuations. This dependency was not systematic and not spatially uniform. Temperature was the most relevant parameter linked with seasonal fluctuation in our study, but it was only significant in three rectangles. This result supports our hypothesis of the annual spawning peak. Higher sea water temperature has been reported during striped red mullet spawning in Israel and Canary Islands (Suquet and Person-Le Ruyet, 2001). For Brittany, striped red mullet spawning is observed in relation with increasing photo-period and temperature(Suquet and Person-Le Ruyet, 2001). One hypothesis is that the second peak may be explained by the recruitment process corresponding to the arrival in the catches of the individuals born the year before. This hypothesis is supported by the fact that biannual abundance seasonality occurs in shallow coastal rectangles and that multiple recruitment peaks have also been observed for different species (see, for example Abella et al. (1995) or Hatfield (1996)). We tried to model the biannual peak of seasonality in striped red mullet abundance with the corresponding peak in environmental covariates but we were not able to link the three coastal rectangles to the same set of environmental variables. One rectangle can be linked to low fluctuation of PC1, one to low fluctuation of PC3 and the third to all variables excepting PC3. The two rectangles where no seasonality was detected are in deep zones. Seasonality of striped red mullet abundance was clearly depth driven. Further studies will be needed to better reveal the link between seasonality in striped red mullet abundance and environmental variables.

A critical issue for a deeper understanding of the dependency of fish abundance on the oceanic variable is the proper definition of space and time scales. The focus was here on the Bay of Biscay over the 2005-2018 period. The Copernicus database used to define environmental covariates revealed a mean increasing trend of surface temperature over the considered period, following a century-long tendency (Garcia-Soto and Pingree, 2012) for the Bay of Biscay. This trend may appear contradictory with the large scale decrease of North Atlantic sea surface temperature noted for instance by Piecuch et al. (2017) over the 2005-2015 period, but is indeed an indicator of the heterogeneity of the ocean dynamics. This underlines that any generalization of local findings should be made with particular caution and vice versa. From an ecological point of view, the use of ICES rectangles to study the impact of the environment on the red mullet population in the Bay of Biscay

raises questions. ICES rectangles correspond to the finest spatial mesh common to the mandatory declarative data of fishermen and not homogeneous ecological units. For example, several habitats may be represented in the same rectangle or conversely, a single habitat may occupy several rectangles. The development of an habitat-delimited analysis will certainly be a fruitful but ambitious and long-term challenge. The present study was strictly bounded by the source data, i.e. by the fishermen's logbooks and fishing forms filled in by ICES rectangle. Moreover there is a crucial need to simultaneously dynamically refine and extend in space and time the mapping of both marine environmental parameters and fish abundance. Developing a model for such a small portion of the ocean is useful to be able to understand the effect of environmental changes on local fisheries. At this scale, most of the fisheries are local small industries. Understanding the link between environment and resources preserves local socio-economic activities, and it is of very high importance. While costly, such an approach appears now to be a prerequisite to decipher the response of marine fauna to the fluctuations of ocean variables. This is already true for the relationships existing at the present time (García-Barón et al., 2020; Véron et al., 2020) and it will become even more necessary to move forward towards a resource-preserving marine spatial planning strategy in the context of global change.

The approach we developed to tackle our applied research question can be applied in a wide range of fish population studies, in order to monitor the effect of climate change on fish population distribution at various scales and tohelp fishermen anticipate changes. The analysis was carried out from abundance time-series, which is the sole information available for a number of natural fish populations. It had also been performed considering the main environmental factors available over the study area, mainly focused in the surface layers. When available, additional factors can be easily implemented and tested such as more complete three-dimensional information (Assis et al., 2016). For the study of striped red mullet, knowledge on benthic habitat composition (Ajemian et al., 2016) or on substrate type (Lombarte et al., 2000; Mahé et al., 2005) can improve the study. Substrate type layer is not yet available for the entire Bay of Biscay. One perspective will be to include new layers in this study, once one is available. Finally, a comprehensive understanding of the time-resolved population dynamics should encompass each driving factor, including trophic web parameters and additional mortality causes.

5. Acknowledgments

Funding was provided by the Energy Environment Solutions (E2S-UPPA) consortium and the BIGCEES project from E2S-UPPA ("Big model and Big data in Computational Ecology and Environmental Sciences"), the Queensland Department of Environment and Science (DES) and the ARC Centre of Excellence for Mathematical and Statistical Frontiers (ACEMS). The data that support the findings of this study is openly available in SEANOE (Kermorvant et al., 2020).
We do not declare any conflict of interest.

6. Tables

Table 1: Main statistical values of two environmental variables (temperature and salinity) recorded over the 2005–2018 period in the selected ICES rectangles. Temperature is expressed in degrees Celcius, salinity in grams of salt per liter of water

		R20E8	**R21E7**	**R21E8**	**R22E7**	**R23E6**	**R23E7**
Salinity	**Min**	28.51	32.36	29.10	31.80	32.27	26.76
	Max	34.65	35.72	34.57	35.53	35.67	34.58
	Med	33.17	34.85	33.12	34.13	34.80	32.10
	Sd	1.27	0.67	0.88	0.66	0.65	1.52
Temperature	**Min**	7.32	8.56	7.09	7.76	8.57	7.32
	Max	22.16	22.54	21.22	21.64	21.52	20.89
	Med	15.26	15.25	14.85	14.84	14.44	14.47
	Sd	4.23	3.77	4.16	3.79	3.34	3.80

Table 2: Results of the linear model to assess the relationship between long term trends of stripped red mullet abundance and environmental variables. Models estimates (β), P-values, R^2 and relative importance (Imp) of variables obtained with linear models on each rectangle. Results with P-values < 0.005 are in bold. Standard deviations of models estimates are available in appendix.

	Type	Intercept	$\widehat{LTT}_{MS}$	$\widehat{LTT}_{MT}$	$\widehat{LTT}_{PC1}$	$\widehat{LTT}_{PC2}$	$\widehat{LTT}_{PC3}$	R^2
R20E8	β	-6.906	0.433	-0.35	0.438	-0.879	0.373	.
	P_value	0.358	**<0.001**	0.219	0.141	0.337	0.611	.
	Imp.	.	0.231	0.246	0.102	0.214	0.069	0.862
R21E7	β	-7.495	0.102	0.205	-0.873	-1.739	1.743	.
	P_value	0.036	0.142	0.1	**<0.001**	**<0.001**	**<0.001**	.
	Imp.	.	0.147	0.308	0.083	0.295	0.069	0.902
R21E8	β	-15.951	0.524	0.071	0.358	-0.731	-0.31	.
	P_value	0.004	**<0.001**	0.772	0.096	0.097	0.67	.
	Imp.	.	0.366	0.163	0.051	0.162	0.087	0.828
R22E7	β	31.395	-0.959	0.177	-0.842	-3.379	2.824	.
	P_value	0.011	**<0.001**	0.618	**<0.001**	**<0.001**	**0.002**	.
	Imp.	.	0.091	0.153	0.077	0.19	0.136	0.647
R23E6	β	-56.003	0.732	1.855	-1.067	-5.673	6.577	.
	P_value	**<0.001**	**0.001**	**<0.001**	**0.003**	**<0.001**	**<0.001**	.
	Imp.	.	0.04	0.214	0.22	0.164	0.254	0.892
R23E7	β	-23.493	0.434	0.632	0.574	-0.922	2.213	.
	P_value	**<0.001**	**<0.001**	**<0.001**	**<0.001**	**<0.001**	**<0.001**	.
	Imp.	.	0.215	0.14	0.207	0.16	0.15	0.8725

Table 3: Results of the linear model to assess the relationship between seasonal trends of stripped red mullet abundance and environmental variables. Model estimates(β), P-values, R^2 and relative importance (Imp) of environmental covariates seasonality in abundance seasonality obtained with lm models on each rectangles. ".12" and ".6" notations correspond to the annual and biannual fluctuations, respectively. Results with p-values < 0.005 are in bold. Standard deviations of models estimates are available in appendix.

	Type	Intercept	$\widehat{ST}_{MS}$	$\widehat{ST}_{MT}$	$\widehat{ST}_{PC1}$	$\widehat{ST}_{PC2}$	$\widehat{ST}_{PC3}$	R^2
R20E8.6	β	0.171	0.063	0.077	-0.365	0.298	0.069	.
	P_value	**<0.001**	0.441	0.031	**<0.001**	0.008	0.598	.
	Imp.	.	0.009	0.119	0.146	0.059	0.051	0.383
R20E8.12	β	-0.167	-0.28	0.278	-0.721	-0.207	0.462	.
	P_value	0.087	**<0.001**	**<0.001**	**<0.001**	0.456	**0.003**	.
	Imp.	.	0.152	0.28	0.272	0.27	0.008	0.982
R21E7.6	β	0.141	-0.271	-0.045	-0.182	0.2	-0.056	.
	P_value	**<0.001**	**0.002**	0.006	**<0.001**	0.007	0.286	.
	Imp.	.	0.167	0.088	0.244	0.075	0.095	0.668
R21E7.12	β	0.232	0.225	-0.141	0.073	0.64	-0.212	.
	P_value	**<0.001**	**<0.001**	0.177	0.571	0.161	0.404	.
	Imp.	.	0.289	0.04	0.034	0.057	0.046	0.466
R21E8.6	β	0.343	-0.765	-0.193	-0.906	0.629	0.024	.
	P_value	**<0.001**	**<0.001**	**<0.001**	**<0.001**	**<0.001**	0.895	.
	Imp.	.	0.261	0.089	0.138	0.069	0.012	0.569
R21E8.12	β	0.227	0.16	-0.25	0.123	-0.018	0.693	.
	P_value	0.011	0.014	**<0.001**	**0.004**	0.877	**<0.001**	.
	Imp.	.	0.144	0.305	0.1	0.266	0.095	0.910
R22E7.6	β	0.152	-0.128	-0.006	0.087	0.092	-0.24	.
	P_value	**<0.001**	0.231	0.82	0.07	0.062	**0.002**	.
	Imp.	.	0.015	0.044	0.021	0.025	0.123	0.229
R22E7.12	β	0.648	0.478	0.37	0.157	-0.973	-1.629	.
	P_value	**<0.001**	0.252	**0.003**	0.253	**<0.001**	**<0.001**	.
	Imp.	.	0.102	0.068	0.027	0.066	0.256	0.520
R23E6.6	β	0.103	-0.026	-0.08	0.26	-0.236	0.24	.
	P_value	0.012	0.897	0.128	0.211	0.253	0.089	.
	Imp.	.	0.008	0.023	0.054	0.012	0.078	0.175
R23E6.12	β	0.403	-0.131	-0.248	1.124	-0.588	-0.092	.
	P_value	**0.003**	0.647	0.026	**<0.001**	**<0.001**	0.456	.
	Imp.	.	0.032	0.243	0.409	0.036	0.241	0.961
R23E7.6	β	0.183	-0.024	0.068	-0.016	-0.076	0.148	.
	P_value	**<0.001**	0.307	**0.001**	0.505	**0.004**	**0.002**	.
	Imp.	.	0.02	0.072	0.007	0.097	0.077	0.273
R23E7.12	β	-0.341	0.025	0.241	-0.228	0.192	-0.106	.
	P_value	**0.002**	0.532	0.029	**0.005**	0.13	0.347	.
	Imp.	.	0.097	0.074	0.131	0.057	0.084	0.442

7. Figure legends

Figure 1: Time-series decomposition in striped red mullet abundance. A: Map of studied rectangles. B, C and D: Long Term Trend ($\widehat{LTT}$), Seasonal Trend (ST) and Residual (R) of $log(LPUE)$ by ICES statistical rectangle, respectively.

Figure 2: Long Term Trends ($\widehat{LTT}$) for striped red mullet abundance and environmental covariates for all studied ICES rectangle. LPUE is landing per unit of effort, expressed in monthly mean of daily kg by rectangle MS is salinity in gram per liter and MT is temperature in degree Celsius, PC1, PC2 and PC3 are the

three first axes of PCA of phytoplankton concentration, chlorophyll concentration, and chemicals variables.
Figure 3: Spectral density of log(LPUE) for each ICES rectangle over the complete time series.
Figure 4: Time-frequency analysis for rectangle R23E7. A: spectral density for $log(LPUE)$ and environmental covariates over the full time-series. B and C: time-resolved magnitude of seasonal fluctuations over a 48-month moving window for biannual and annual components, respectively, for $log(LPUE)$ and environmental covariates. MS is salinity in gram per liter and MT is temperature in degree Celsius, PC1, PC2 and PC3 are the three first axes of PCA of phytoplankton concentration, chlorophyll concentration, and chemicals variables.

References

Abella, A., Auteri, R., Serena, F., 1995. Some aspects of growth and recruitment of hake in the northern tyrrhenian sea. Rapport Commision International Mer Méditerranée 34, 235.

Ajemian, M., Kenworthy, M., Sánchez-Lizaso, J.L., Cebrián, J., 2016. Aggregation dynamics and foraging behaviour of striped red mullet *Mullus surmuletus* in the western mediterranean sea. Journal of fish biology 88, 2051–2059. doi:10.1111/jfb.12932.

Araujo, M.B., Guisan, A., 2006. Five (or so) challenges for species distribution modelling. Journal of biogeography 33, 1677–1688. doi:10.1111/j.1365-2699.2006.01584.x.

Assis, J., Coelho, N.C., Lamy, T., Valero, M., Alberto, F., Serrão, E.Á., 2016. Deep reefs are climatic refugia for genetic diversity of marine forests. Journal of biogeography 43, 833–844. doi:10.1111/jbi.12677.

Beare, D., Burns, F., Jones, E., Peach, K., Reid, D., 2005. Red mullet migration into the northern north sea during late winter. Journal of Sea Research 53, 205–212. doi:10.1016/j.seares.2004.06.003.

Beare, D., McKenzie, E., 1999. Connecting ecological and physical time-series: the potential role of changing seasonality. Marine Ecology Progress Series 178, 307–309.

Bentlage, B., Peterson, A.T., Barve, N., Cartwright, P., 2013. Plumbing the depths: extending ecological niche modelling and species distribution modelling in three dimensions. Global Ecology and Biogeography 22, 952–961. doi:10.1111/geb.12049.

Bloomfield, P., 2004. Fourier analysis of time series: an introduction. John Wiley & Sons.

Both, C., Bouwhuis, S., Lessells, C., Visser, M.E., 2006. Climate change and population declines in a long-distance migratory bird. Nature 441, 81–83. doi:10.1038/nature04539.

Box, E.E., 2012. Macroclimate and plant forms: an introduction to predictive modeling in phytogeography. volume 1. Springer Science & Business Media.

Brander, K., 2010. Impacts of climate change on fisheries. Journal of Marine Systems 79, 389–402. doi:10.1016/j.jmarsys.2008.12.015.

Brockwell, P.J., Davis, R.A., Fienberg, S.E., 1991. Time series: theory and methods: theory and methods. Springer Science & Business Media.

Broekhuizen, N., McKenzie, E., 1995. Patterns of abundance for calanus and smaller copepods in the north sea: time series decomposition of two cpr data sets. Marine ecology progress series. Oldendorf 118, 103–120. doi:10.3354/meps118103.

Caill-Milly, N., Lissardy, M., Bru, N., Dutertre, M.A., Saguet, C., 2019. A methodology based on data filtering to identify reference fleets to account for the abundance of fish species: Application to the striped red mullet *(Mullus surmulletus)* in the bay of biscay. Continental Shelf Research doi:10.1016/j.csr.2019.06.004.

Castelle, B., Dodet, G., Masselink, G., Scott, T., 2017. A new climate index controlling winter wave activity along the atlantic coast of europe: The west europe pressure anomaly. Geophysical Research Letters 44, 1384–1392. doi:10.1002/2016GL072379.

Cohen, J.M., Lajeunesse, M.J., Rohr, J.R., 2018. A global synthesis of animal phenological responses to climate change. Nature Climate Change 8, 224–228. doi:10.1038/s41558-018-0067-3.

Costello, C., Ovando, D., Hilborn, R., Gaines, S.D., Deschenes, O., Lester, S.E., 2012. Status and solutions for the world's unassessed fisheries. Science 338, 517–520. doi:10.1126/science.1223389.

deCastro, M., Gómez-Gesteira, M., Alvarez, I., Gesteira, J., 2009. Present warming within the context of cooling–warming cycles observed since 1854 in the bay of biscay. Continental Shelf Research 29, 1053 – 1059. doi:10.1016/j.csr.2008.11.016. 100 Years of Research within the Bay of Biscay.

Desbrosses, P., 1935. Contribution à la connaissance de la biologie du rouget barbet en atlantique nord (iii). M. barbatus , 351–376.

Dowling, N.A., Smith, A.D., Smith, D.C., Parma, A.M., Dichmont, C.M., Sainsbury, K., Wilson, J.R., Dougherty, D.T., Cope, J.M., 2019. Generic solutions for data-limited fishery assessments are not so simple. Fish and Fisheries 20, 174–188. doi:10.1111/faf.12329.

Ferguson, C., Carvalho, L., Scott, E., Bowman, A., Kirika, A., 2008. Assessing ecological responses to environmental change using statistical models. Journal of Applied Ecology 45, 193–203. doi:10.1111/j.1365-2664.2007.01428.x.

Franklin, J., Wejnert, K.E., Hathaway, S.A., Rochester, C.J., Fisher, R.N., 2009. Effect of species rarity on the accuracy of species distribution models for reptiles and amphibians in southern california. Diversity and distributions 15, 167–177. doi:10.1111/j.1472-4642.2008.00536.x.

Free, C.M., Thorson, J.T., Pinsky, M.L., Oken, K.L., Wiedenmann, J., Jensen, O.P., 2019. Impacts of historical warming on marine fisheries production. Science 363, 979–983. doi:10.1126/science.aau1758.

Frei, C., Schöll, R., Fukutome, S., Schmidli, J., Vidale, P.L., 2006. Future change of precipitation extremes in europe: Intercomparison of scenarios from regional climate models. Journal of Geophysical Research: Atmospheres 111. doi:10.1029/2005JD005965.

García-Barón, I., Santos, M.B., Saavedra, C., Astarloa, A., Valeiras, J., Barcelona, S.G., Louzao, M., 2020. Essential ocean variables and high value biodiversity areas: Targets for the conservation of marine megafauna. Ecological Indicators 117, 106504.

García-Rodríguez, M., Fernández, A., Esteban, A., 2011. Biomass response to environmental factors in two congeneric species of mullus, *M. barbatus* and *M. surmuletus*, off catalano-levantine mediterranean coast of spain: a preliminary approach. Animal Biodiversity and Conservation 34, 113–122.

García-Rubies, A., Macpherson, E., 1995. Substrate use and temporal pattern of recruitment in juvenile fishes of the mediterranean littoral. Marine biology 124, 35–42. doi:10.1007/BF00349144.

Garcia-Soto, C., Pingree, R.D., 2012. Atlantic multidecadal oscillation (amo) and sea surface temperature in the bay of biscay and adjacent regions. Marine Biological Association of the United Kingdom. Journal of the Marine Biological Association of the United Kingdom 92, 213.

Grömping, U., et al., 2006. Relative importance for linear regression in r: the package relaimpo. Journal of statistical software 17, 1–27. doi:10.18637/jss.v017.i01.

Hatfield, E.M., 1996. Towards resolving multiple recruitment into loliginid fisheries: Loligo gahi in the falkland islands fishery. ICES Journal of Marine Science 53, 565–575.

Hess, Iyer, M., 2001. Linear trend analysis: a comparison of methods. Atmospheric Environment 35, 5211–5222. doi:10.1016/S1352-2310(01)00342-9.

Hsieh, C.H., Chen, C.S., Chiu, T.S., Lee, K.T., Shieh, F.J., Pan, J.Y., Lee, M.A., 2009. Time series analyses reveal transient relationships between abundance of larval anchovy and environmental variables in the coastal waters southwest of taiwan. Fisheries Oceanography 18, 102–117. doi:10.1111/j.1365-2419.2008.00498.x.

Huang, N.E., Shen, Z., Long, S.R., Wu, M.C., Shih, H.H., Zheng, Q., Yen, N.C., Tung, C.C., Liu, H.H., 1998. The empirical mode decomposition and the hilbert spectrum for nonlinear and non-stationary time series analysis. Proceedings of the Royal Society of London. Series A: mathematical, physical and engineering sciences 454, 90–995. doi:10.1098/rspa.1998.0193.

Hulme, M., 2002. Climate change scenarios for the United Kingdom: the UKCIP02 scientific report. Tyndall Centre for Climate Mental Sciences University.

Huntley, B., Berry, P.M., Cramer, W., McDonald, A.P., 1995. Special paper: modelling present and potential future ranges of some european higher plants using climate response surfaces. Journal of Biogeography , 967–1001doi:10.2307/2845830.

Hurrell, J.W., 1995. Decadal trends in the north atlantic oscillation: regional temperatures and precipitation. Science 269, 676–679. doi:10.1126/science.269.5224.676.

Hyndman, R., Athanasopoulos, G., 2018. Forecasting: Principles and Practice, 2nd edition. OTexts: Melbourne, Australia.

ICES, 2012. ICES Implementation of Advice for Data-limited Stocks in 2012 in its 2012 Advice. Technical Report ICES CM 2012/ACOM 68. doi:10.17895/ices.pub.5322.

ICES, 2019. Working Group on Widely Distributed Stocks (WGWIDE). Technical Report ICES Scientific Reports 1:36. doi:10.17895/ices.pub.5574.

ICES, 2020. Striped red mullet (Mullus surmuletus) in subareas 6 and 8, and divisions 7.a–c, 7.e–k, and 9.a (North Sea, Bay of Biscay, southern Celtic Seas, and Atlantic Iberian waters).. International Council for the Exploration of the Sea (ICES)", doi = https://doi.org/10.17895/ices.advice.5772.

IPCC, 2007. Climate Change 2007: the physical science basis. volume 996. Cambridge University Press.

Kearney, M., Porter, W., 2009. Mechanistic niche modelling: combining physiological and spatial data to predict species' ranges. Ecology letters 12, 334–350. doi:10.1111/j.1461-0248.2008.01277.x.

Kermorvant, C., Caill-Milly, N., Sous, D., Paradinas, I., Lissardy, M., Liquet, B., 2020. Dataset : Striped red mullet landing per unit of effort and environmental variables in the bay of biscay. SEANOE doi:https://doi.org/10.17882/77179.

Kousteni, V., Anastasopoulou, A., Mytilineou, C., 2019. Life-history traits of the striped red mullet mullus surmuletus (linnaeus, 1758) in the south aegean sea (eastern mediterranean). Journal of the Marine Biological Association of the United Kingdom 99, 1417–1427. doi:10.1017/S0025315419000353.

Koutsikopoulos, C., Beillois, P., Leroy, C., Taillefer, F., 1998. Temporal trends and spatial structures of the sea surface temperature in the bay of biscay. Oceanologica Acta 21, 335 – 344. doi:10.1016/S0399-1784(98)80020-0. international Conference on Oceanography of the Bay of Biscay.

Labropoulou, M., Machias, A., Tsimenides, N., Eleftheriou, A., 1997. Feeding habits and ontogenetic diet shift of the striped red mullet, *Mullus surmuletus* linnaeus, 1758. Fisheries Research 31, 257–267. doi:10.1016/S0165-7836(97)00017-9.

Lart, W.B., 2019. Guide to Data-limited stock assessment. Technical Report Seafish Report 744. Sea Fish Industry Authority.

Le Quesne, W., Brown, M., De Oliveira, J., Casey, J., O'Brien, C., 2013. Data-deficient fisheries in eu waters. directorate-general for internal policies, policy department b: Structural and cohesion policies. Fisheries. IP/B/PECH/IC/2012–118 , 7.

Leaute, J.P., Caill-Milly, N., Lissardy, N., Dutertre, M.A., Saguet, C., 2018. ROMELIGO. Amélioration des connaissances halieutiques du ROuget-barbet, du MErlan et du LIeu jaune du GOlfe de Gascogne. Technical Report.

Lentka, , Smulko, J., 2019. Methods of trend removal in electrochemical noise data – overview. Measurement 131, 569–581. doi:10.1016/j.measurement.2018.08.023.

Lombarte, A., Recasens, L., González, M., de Sola, L.G., 2000. Spatial segregation of two species of mullidae (*Mullus surmuletus* and *Mullus barbatus*) in relation to habitat. Marine Ecology Progress Series 206, 239–249. doi:10.3354/meps206239.

Machias, A., Labropoulou, M., 2002. Intra-specific variation in resource use by red mullet, mullus barbatus. Estuarine, Coastal and Shelf Science 55, 565 – 578. doi:https://doi.org/10.1006/ecss.2001.0924.

Maes, J., Stevens, M., Breine, J., 2007. Modelling the migration opportunities of diadromous fish species along a gradient of dissolved oxygen concentration in a european tidal watershed. Estuarine, Coastal and Shelf Science 75, 151–162. doi:10.1016/j.ecss.2007.03.036.

Mahé, K., Destombes, A., Coppin, F., Koubbi, P., Vaz, S., Le Roy, D., Carpentier, A., 2005. Le rouget barbet de roche *Mullus surmuletus* (l. 1758) en manche orientale et mer du nord. Rapport de Contrat IFREMER/CRPMEM Nord-Pas-de-Calais .

Mahe, K., Villanueva, M.C., Vaz, S., Coppin, F., Koubbi, P., Carpentier, A., 2014. Morphological variability of the shape of striped red mullet mullus surmuletus in relation to stock discrimination between the bay of biscay and the eastern english channel. Journal of Fish Biology 84, 1063–1073. doi:10.1111/jfb.12345.

Maravelias, C.D., Tsitsika, E.V., Papaconstantinou, C., 2007. Environmental influences on the spatial distribution of european hake (*Merluccius merluccius*) and red mullet (*Mullus barbatus*) in the mediterranean. Ecological Research 22, 678–685. doi:10.1007/s11284-006-0309-0.

Mateo, M., Pawlowski, L., Robert, M., 2016. Highly mixed fisheries: fine-scale spatial patterns in retained catches of french fisheries in the celtic sea. ICES Journal of Marine Science 74, 91–101. doi:10.1093/icesjms/fsw129.

McCarty, J.J., Canziani, O., Leary, N., Dokken, D., White, K., 2001. Climate change 2001: impacts, adaptation, and vulnerability. Contribution of working group II to the Third assessment report of the intergovernmental panel on climate change. Technical Report. Cambridge University Press.

Melo-Merino, S.M., Reyes-Bonilla, H., Lira-Noriega, A., 2020. Ecological niche models and species distribution models in marine environments: A literature review and spatial analysis of evidence. Ecological Modelling 415, 108837. doi:10.1016/j.ecolmodel.2019.108837.

N'Da, K., Déniel, C., 1993. Sexual cycle and seasonal changes in the ovary of the red mullet, *Mullus surmuletus*, from the southern coast of brittany. Journal of fish biology 43, 229–244. doi:10.1111/j.1095-8649.1993.tb00425.x.

Oskarsson, G.J., Aldrin, M., Bal, G., Berge, B., Beukhof, E.D., Björnsson, H., Brunel, T., Burns, F., Campbell, A., Campbell, N., et al., 2019. Working Group on Widely Distributed Stocks (WGWIDE). Technical Report.

Pajuelo, J., Lorenzo, J., Ramos, A., Méndez-Villamil, M., 1997. Biology of the red mullet mullus surmuletus (mullidae) off the canary islands, central-east atlantic. African Journal of Marine Science 18.

Peck, M., Pinnegar, J.K., 2019. Climate change impacts, vulnerabilities and adaptations: North atlantic and atlantic arctic marine fisheries. Impacts of climate change on fisheries and aquaculture , 87.

Peterson, A.T., Papeş, M., Soberón, J., 2015. Mechanistic and correlative models of ecological niches. European Journal of Ecology 1, 28–38. doi:10.1515/eje-2015-0014.

Piecuch, C.G., Ponte, R.M., Little, C.M., Buckley, M.W., Fukumori, I., 2017. Mechanisms underlying recent decadal changes in subpolar n orth a tlantic o cean heat content. Journal of Geophysical Research: Oceans 122, 7181–7197.

Planque, B., Beillois, P., Jégou, A.M., Lazure, P., Petitgas, P., Puillat, I., 2003. Large-scale hydroclimatic variability in the bay of biscay: the 1990s in the context of interdecadal changes, in: ICES Marine Science Symposia, pp. 61–70.

Plaza, F., Salas, R., Yáñez, E., 2018. Identifying ecosystem patterns from time series of anchovy (engraulis ringens) and sardine (sardinops sagax) landings in northern chile. Journal of Statistical Computation and Simulation 88, 1863–1881. doi:10.1080/00949655.2017.1410150.

Potts, S.E., Rose, K.A., 2018. Evaluation of glm and gam for estimating population indices from fishery independent surveys. Fisheries Research 208, 167–178. doi:10.1016/j.fishres.2018.07.016.

Puillat, I., Lazure, P., Jegou, A.M., Lampert, L., Miller, P., 2006. Mesoscale hydrological variability induced by northwesterly wind on the french continental shelf of the bay of biscay. Scientia Marina 70, 15–26. doi:10.3989/scimar.2006.70s115.

Reñones, O., Massuti, E., Morales-Nin, B., 1995. Life history of the red mullet mullus surmuletus from the bottom-trawl fishery off the island of majorca (north-west mediterranean). Marine Biology 123, 411–419. doi:10.1007/BF00349219.

Rijnsdorp, A.D., Peck, M.A., Engelhard, G.H., Möllmann, C., Pinnegar, J.K., 2009. Resolving the effect of climate change on fish populations. ICES journal of marine science 66, 1570–1583. doi:10.1093/icesjms/fsp056.

Roessig, J.M., Woodley, C.M., Cech, J.J., Hansen, L.J., 2004. Effects of global climate change on marine and estuarine fishes and fisheries. Reviews in fish biology and fisheries 14, 251–275. doi:10.1007/s11160-004-6749-0.

SACROIS, . Sacrois website. `http://sih.ifremer.fr/Description-des-donnees/Les-donnees-estimees/SACROIS`.

Sakamoto, Y., Ishiguro, M., Kitagawa, G., 1986. Akaike information criterion statistics. Dordrecht, The Netherlands: D. Reidel 81. doi:10.1080/01621459.1988.10478680.

Shumway, R.H., Stoffer, D.S., 2017. Time series analysis and its applications: with R examples. Springer.

Stoica, P., Moses, R.L., et al., 2005. Spectral analysis of signals. Pearson Prentice Hall Upper Saddle River, NJ.

Stott, P.A., Sutton, R.T., Smith, D.M., 2008. Detection and attribution of atlantic salinity changes. Geophysical Research Letters 35. doi:10.1029/2008GL035874.

Suquet, M., Person-Le Ruyet, J., 2001. Les rougets barbets (*Mullus barbatus*, *Mullus surmuletus*): biologie, pêche, marché et potentiel aquacole. Editions Quae.

Vaz, S., Carpentier, A., Coppin, F., 2004. Eastern english channel fish community from 1988 to 2003 and its relation to the environment. ICES CM 2004, 40.

Véron, M., Duhamel, E., Bertignac, M., Pawlowski, L., Huret, M., 2020. Major changes in sardine growth and body condition in the bay of biscay between 2003 and 2016: Temporal trends and drivers. Progress in Oceanography 182, 102274.

Wood, S.N., 2017. Generalized additive models: an introduction with R. CRC press.

Young, P.C., Pedregal, D.J., Tych, W., 1999. Dynamic harmonic regression. Journal of forecasting 18, 369–394. doi:10.1002/(SICI)1099-131X(199911)18:6¡369::AID-FOR748¿3.0.CO;2-K.